

Symmetry-breaking Ta⁴⁺ centers in KTaO₃

V. V. Laguta, M. I. Zaritskii, M. D. Glinchuk, and I. P. Bykov

Institute for Problem of Material Sciences, Ukrainian Academy of Sciences, Krgiganovskogo 3, 252180 Kiev, Ukraine

J. Rosa and L. Jastrabík

Institute of Physics, Academy of Sciences of the Czech Republic, Cukrovarnická 10, 16253 Prague, Czech Republic

(Received 29 October 1997)

A study of photoinduced Ta⁴⁺ centers in nominally pure KTaO₃ single crystals has been carried out by electron-spin resonance. Two of these centers (Ta⁴⁺-V_O and Ta⁴⁺-V_O-Me⁴⁺) are connected with vacancies of oxygen (V_O); a third center is associated with an OH⁻ molecular ion (Ta⁴⁺-OH⁻). This assignment is made on the basis of concentration measurements of the corresponding centers after annealing in argon, oxygen, hydrogen, and H₂O vapor atmospheres. It has been shown that the Ta⁴⁺ centers are shallow donors; at $T \geq 30$ K they are ionized and transformed into ordinary V_O and OH⁻ which are assumed to be the main lattice defects before illumination. Their energy levels are determined by the temperature dependence of the relaxation rate of the light-induced nonequilibrium localized electron population. The energy levels of Ta⁴⁺-V_O and Ta⁴⁺-V_O-Me⁴⁺ centers are situated at 26 and 8 meV below the bottom of the conduction band, respectively. The symmetry of the centers is inverse broken in the sense that the photoelectron is localized near one of two equivalent Ta⁵⁺ ions next to an oxygen vacancy or OH⁻. The role of V_O defects and OH⁻ molecules in the nucleation of local polar clusters in nominally pure KTaO₃ crystals at low temperatures is discussed. [S0163-1829(98)00225-2]

I. INTRODUCTION

The anomalous low-temperature properties of nominally pure incipient ferroelectric KTaO₃ have attracted much attention from scientists in the last few years. However, the origin and driving forces of these anomalies have not been clear up to now. Since the property anomalies at $T < 50$ K were shown to be sample dependent, many defects and unavoidable impurities were discussed as possible reasons for these anomalies. For example, some recently revealed^{1,2} impurities in nominally pure (undoped) KTaO₃ were shown to be symmetry-breaking impurities which are able to induce local polar clusters of correlation radius size $r_c \approx 20-50$ Å at $T < 50$ K. These clusters can be the source of an inversion center disappearance in part of the crystal volume, which makes it possible to observe second harmonic generation (SHG),³ first-order Raman scattering (FOR),⁴ dielectric losses,⁵ etc.

In crystals annealed in a hydrogen atmosphere, enhanced SHG and FOR spectra and other phenomena were revealed and discussed recently⁶⁻¹⁰ as manifestations of oxygen vacancies. It is clear that a "pure" oxygen vacancy V_O is unable to destruct inversion symmetry, i.e., to be the source of a polar cluster. It was suggested that Ta³⁺-V_O could be the origin of the polar microregions.^{6,7} This was done on the basis of Raman and fluorescence measurements exhibiting a sharp zero-phonon-like emission near 687 nm. However, a comparative study⁹ of crystals from different laboratories revealed no correlation between this luminescence at 687 nm and several other quantities like FOR or SHG. On the other hand, the increased intensity of FOR (Ref. 7) and SHG (Ref. 10) after annealing in a H₂ atmosphere does give some hints on the connection of the aforementioned phenomena with lattice vacancies and maybe with OH⁻ groups, which are

known to penetrate easily into the crystal under such conditions.¹¹ In spite of much effort both in experimental and theoretical investigations of the microscopic structure of defects, which are the sources of local polar clusters in KTaO₃, the situation has not been clear up to now. Therefore, the continuation of thorough studies of lattice defects like oxygen vacancies and the surrounding lattice distortion, as well as the influence of light on these centers, seems to be extremely important.

It should be emphasized that oxygen vacancy centers with different ionization levels and near-neighbor distortions were assumed earlier¹² to be shallow donors. Such donors might form an impurity band overlapping with the conduction band and creating conductivity down to very low temperatures. On the other hand, the observation of high photoconductivity at $T < 70$ K without any high-temperature treatment, like that revealed recently in K_{1-x}Li_xTaO₃,¹³ speaks in favor of strong light influence on the local electronic structure of these materials.

In the present work we have carried out electron-spin-resonance (ESR) investigations of photoinduced Ta⁴⁺ centers situated near different lattice defects such as oxygen vacancies, OH⁻ ions, and substitutional impurities. The temperature regions of center stability and the local electronic levels have been determined. An investigation of the influence of sample annealing in Ar, O₂, H₂O, and H₂ atmospheres on ESR spectra made it possible to propose the Ta⁴⁺ center models and the mechanism of their creation. The roles of oxygen vacancies and OH⁻ molecules, both in the nucleation of local polar clusters and in other peculiarities of nominally pure KTaO₃ single crystals, have been discussed.

II. SAMPLES AND EXPERIMENTAL DETAILS

The measurements were carried out on single-crystal samples of KTaO₃ both nominally pure and slightly doped

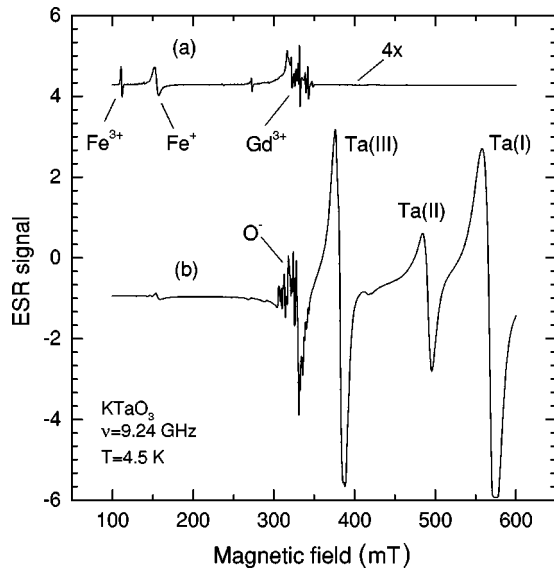


FIG. 1. ESR spectra for $B \parallel \langle 100 \rangle$ before (a) and after (b) illumination in nominally pure KTaO_3 . Ta(I), Ta(II), and Ta(III) denote the spectra of Ta^{4+} centers. Signal amplification is four times higher for spectrum (a) than for spectrum (b).

with Fe and Cr (~ 100 ppm). Two different methods have been used to grow KTaO_3 crystals: the spontaneous crystallization technique, and the Czochralski method. The starting components were K_2CO_3 and Ta_2O_5 of high purity, i.e., the content of unavoidable impurities was less than 10–50 ppm. All of the crystals were colorless. The specimen dimensions were $1 \times 2 \times 3 \text{ mm}^3$, with the surfaces parallel to crystallographic (100) planes.

ESR spectra were recorded in the X-band microwave region. The Oxford Instruments ESR-9 cryosystem allowed us to measure in the temperature range 4.2–77 K with an accuracy of 0.1–0.2 K. An arc lamp of 200 W power served as the source of the light beam. Optical filters made it possible to extract lines with wavelengths of 365, 405, 436, 546, and 577 nm. The samples were illuminated in the resonator through a system of optical lenses, and a special window in the resonator wall.

III. EXPERIMENTAL RESULTS AND THEIR INTERPRETATION

A. Electron-spin-resonance spectra

Studies of nonphotoinduced paramagnetic centers in KTaO_3 have been carried out by us earlier.^{1,2} In nominally pure samples we found $\text{Fe}_{ax}^{3+}(\text{K})$ and $\text{Fe}_{ax}^+(\text{K})$ centers of axial symmetry and $\text{Gd}_c^{3+}(\text{K})$ centers of cubic symmetry. In chromium doped specimens, we have revealed $\text{Cr}^+(\text{K})$ and $\text{Cr}^{5+}(\text{Ta})$ spectra.¹⁴

After illumination by light with $\lambda = 365$ nm at $T = 4.5$ K, ESR signals arise (see Fig. 1). Qualitatively these spectra do not depend on whether the KTaO_3 crystals are nominally pure, or slightly Fe or Cr doped. Thus these spectra were observable in all kinds of samples under investigation. Photoinduced spectra became unobservable only in samples which were strongly doped with iron or some other impurities.

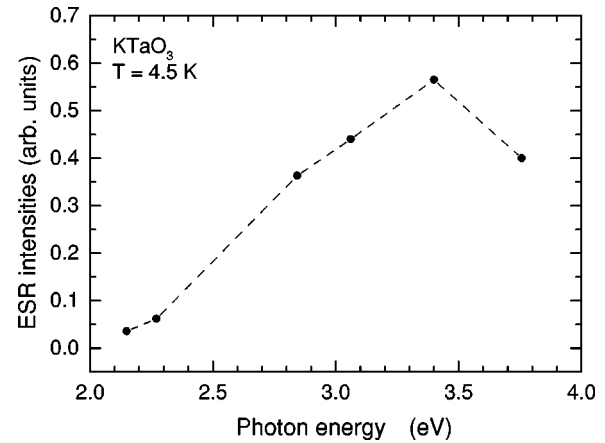


FIG. 2. The dependence of ESR intensity of Ta^{4+} centers on the photon energy.

The intensity of photoinduced spectra depends on the photon energy (Fig. 2). The intensity begins to decrease from $\lambda = 365$ nm (3.4 eV), and at $\lambda = 577$ nm (2.15 eV) it decreased about 20 times.

The observed ESR lines can be divided into two groups. The first one has g -factor values in the range from 2.01 to 2.11. This spectrum was described and analyzed in detail in Ref. 15, where it was shown to belong to paramagnetic O^- centers. In this paper we are interested in another group of ESR lines in the higher-magnetic-field region. This group includes three spectra. We suggest that they belong to Ta^{4+} ($5d^1$, $S = \frac{1}{2}$) ions with different surroundings. The following experimental data prove our assumption.

First, the spectra were more intensive by several orders than spectra of any paramagnetic impurity in nominally pure KTaO_3 investigated earlier (Fig. 1 and Ref. 1). Despite their different histories (the samples were fabricated in different labs by various techniques, so that they contained different amounts and types of defects), such spectra were observed in all of the crystals under investigation. The huge intensity of these photoinduced spectra convinces us that they are possibly connected with host ions of the lattice. The ESR lines of all these spectra have approximately the same large width of

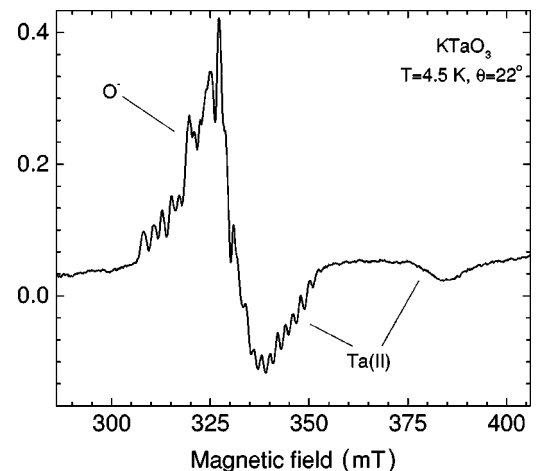


FIG. 3. The ESR spectrum of Ta(II) (assumed to be a $\text{Ta}^{4+} - \text{OH}^-$ center) with a hyperfine structure caused by the ^{181}Ta isotope.

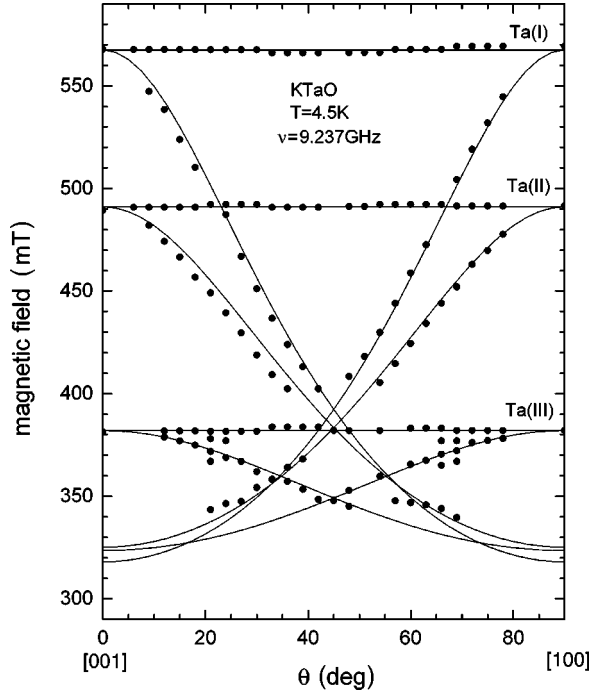


FIG. 4. The angular dependence of Ta^{4+} resonance fields (solid lines, theory; points, experiment).

$\Delta B \approx 14$ mT originating from unresolved hyperfine and superhyperfine interactions. The hyperfine interaction caused by the ^{181}Ta nucleus ($I = \frac{7}{2}$, 100% abundance) was resolved only for the Ta(II) spectrum (Fig. 3).

All spectra show an axial symmetry along $\langle 001 \rangle$ directions, and can be described by a spin Hamiltonian $\mathcal{H} = \mu_B \mathbf{B} g \mathbf{S}$ with $S = \frac{1}{2}$. The complete angular dependence of the resonance fields and their theoretical fitting are depicted in Fig. 4. The spectral parameters of the centers are gathered in Table I. It is seen that the g -tensor components are typical of d^1 ions in an octahedral ligand field with tetragonal distortion.¹⁶ For this case, using the crystal-field model, the g factors can be represented by the expressions

$$g_{\parallel} = g_e - \frac{8\lambda}{\Delta}, \quad g_{\perp} = g_e - \frac{2\lambda}{\delta}. \quad (3.1)$$

Here $g_e = 2.0023$, λ is the spin-orbit coupling constant, and Δ and δ denote the values of the electronic level split-

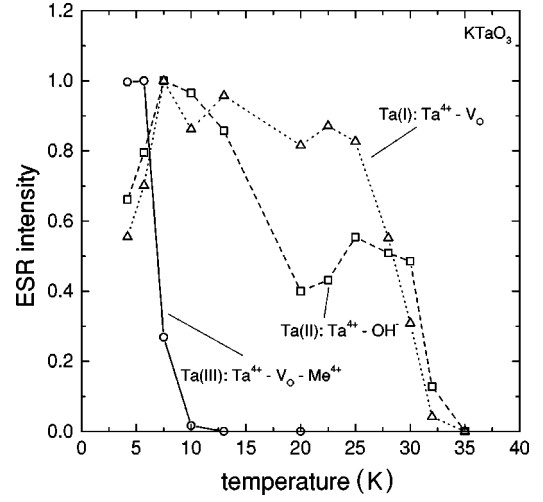


FIG. 5. The temperature dependence of the ESR intensity of Ta^{4+} centers, determined by isochronal anneal, after illumination at 4.5 K.

tings in an octahedral crystal field with tetragonal distortion. The sequence $g_{\parallel} > g_{\perp}$ points to an xy ground state of the T_2 orbital triplet.

Note that g_{\parallel} is slightly larger than g_e for all Ta^{4+} centers. This is usually observed in many oxygen perovskites due to the covalency effect, which has to be calculated out of the crystal-field model. Moreover, the covalency effect becomes progressively more important as the charge of the paramagnetic ion increases. The resultant transfer of charge to the ligands lowers the effective value of the spin-orbit coupling, and may increasingly change the expected magnitudes of g components. Such behavior was observed for $3d^3$ ions in $SrTiO_3$,¹⁷ and in particular for Fe^{5+} a value of $g = 2.013$ was obtained. Note that, for Ti^{3+} in $KTaO_3$, $g_{\parallel} = 1.997$,¹⁸ which is already less than g_e . On the other hand, the proximity of g_{\parallel} values to g_e in $KTaO_3$ can be due to the large octahedral crystal field, which is much larger than that in $BaTiO_3$.

B. Thermal stability and energy levels of Ta^{4+} centers

For the investigation of thermal stability of the centers, we used the method of isochronal annealing, i.e., we heated the sample to a given temperature, held it for one minute, and then quickly cooled it down to 4.5 K, where ESR was measured. The obtained signal heights are depicted in Fig. 5.

TABLE I. ESR spectral parameters of Ta^{4+} centers in $KTaO_3$.

Center	T (K)	g -factor	A (10^{-4} cm^{-1})	Temperature stability
Ta(I): $Ta^{4+} - V_O$	4.5	$g_{\parallel} = 2.07(1)$ $g_{\perp} = 1.163(2)$		Annealed at 30 K $E = 26(4)$ meV
Ta(II): $Ta^{4+} - OH^-$	4.5	$g_{\parallel} = 2.03(1)$ $g_{\perp} = 1.344(2)$	20(5)	Annealed at 30 K
Ta(III): $Ta^{4+} - V_O - Me^{4+}$	4.5	$g_{\parallel} = 2.04(2)$ $g_{\perp} = 1.728(3)$		Annealed at 7 K $E = 8(1)$ meV

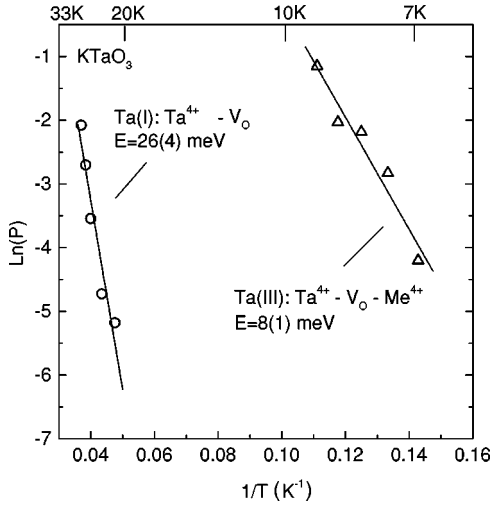


FIG. 6. The temperature dependence of the ionization probability of Ta⁴⁺ centers.

It can be seen that Ta⁴⁺ centers are very shallow; their spectra disappear after heating the sample up to 30 K.

The fact that the Ta⁴⁺ centers are thermally ionized at low temperatures suggests that their energy levels are close to the conduction-band bottom built from *d* states of Ta atoms. These level positions were obtained from measurements of the center ionization probability which is usually expressed in the form of Arrhenius law¹⁹

$$P = N_c v S \exp\left(-\frac{E}{kT}\right). \quad (3.2)$$

N_c is the effective density of states in the conduction band, and v and S are the electron thermal velocity and cross section of its capture, respectively. The value of P at any temperature can be obtained from measurement of the time decay of localized carrier concentration after switching off the light. If one neglects the possibility of the carriers recapture, the concentration decay rate can be described by

$$\frac{dn}{dt} = -nP. \quad (3.3)$$

The solution of Eq. (3.3) gives an exponential dependence of the concentration of localized electrons on time,

$$n = n_0 e^{-Pt}, \quad (3.4)$$

which was indeed observed in our measurements. In simple cases, the effective density of states in the conduction band is proportional to $T^{3/2}$, $v \sim T^{1/2}$, and S is temperature independent. Thus the product $N_c v S$ can be estimated to be at most proportional to T^2 . Therefore, the temperature dependence of the center ionization probability is mainly determined by the exponent in Eq. (3.2). The results of experimental data analysis are given in Fig. 6, where the slopes of lines give us the energies of the electronic levels. The temperature dependence of the pre-exponential factor was neglected because its exact form is not clear for the considered case, and a factor like T^2 can lead to a mere 15–20 % decrease of the ionization energies. In Fig. 6, we depict the data for Ta(I) and Ta(III) centers only. This is because it appeared difficult to

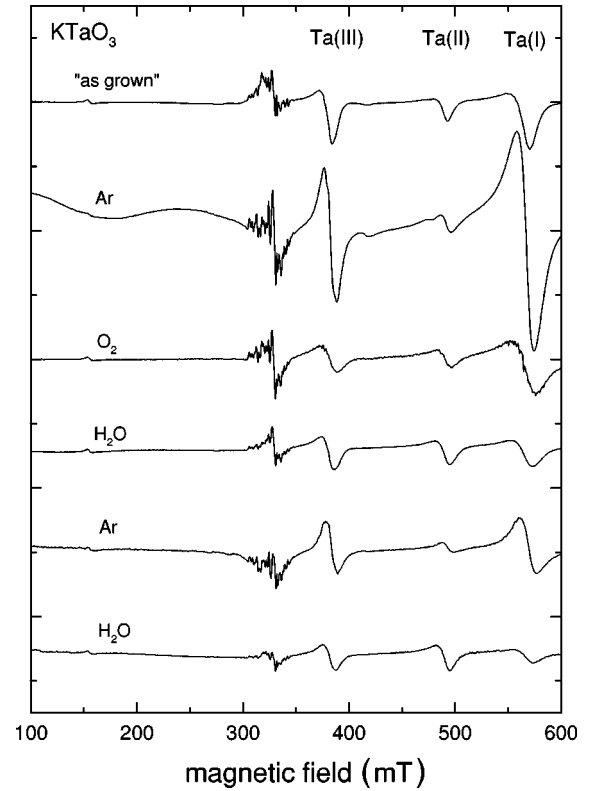


FIG. 7. The dependence of ESR spectra of Ta⁴⁺ centers on the annealing of KTaO₃ in Ar, O₂, and H₂O atmospheres.

determine the energy-level position of the Ta(II) center by the same method due to the strong decay of its ESR signal at $T \approx 15$ K (see Fig. 5). We only can say that the electronic level of Ta(II) may be close to that of Ta(I), because the ESR signals of these centers disappear at the same temperatures.

C. Influence of high-temperature annealing on Ta⁴⁺ centers

It seems to be obvious that a localized state like Ta⁴⁺ can appear only in the vicinity of some lattice defects, e.g., a vacancy of oxygen or the impurity ion. Note that there is information in the literature about polaronic states for B ions, namely, about Ti³⁺ in BaTiO₃.²⁰ As mentioned earlier, such lattice defects could be vacancies of oxygen and OH⁻ molecules, which are known to be unavoidable defects in KTaO₃. To find out whether these defects are really connected with Ta⁴⁺ centers, we have performed annealing of the samples in different gas atmospheres, namely Ar, O₂, and H₂O vapors at $T = 1000$ °C during a time of 3 h. The samples were heated and cooled with a velocity of 10 °C/min. The ESR spectra were recorded at a temperature $T = 4.2$ K. We chose the annealing duration 2–4 h as an optimal one to conserve the reversibility of ESR spectra after the annealing process. When the duration of annealing was longer than 5–6 h, it appeared impossible to recover the spectra after annealing due to ion recharging and the appearance of strong electric conductivity. The results of measurements are depicted in Figs. 7 and 8. It is seen that the behavior of centers Ta(I) and Ta(III) is almost the same for different annealing atmospheres. The ESR line intensities of these centers strongly increased after annealing in inert gas Ar, and decreased at subsequent annealing in O₂ and H₂O

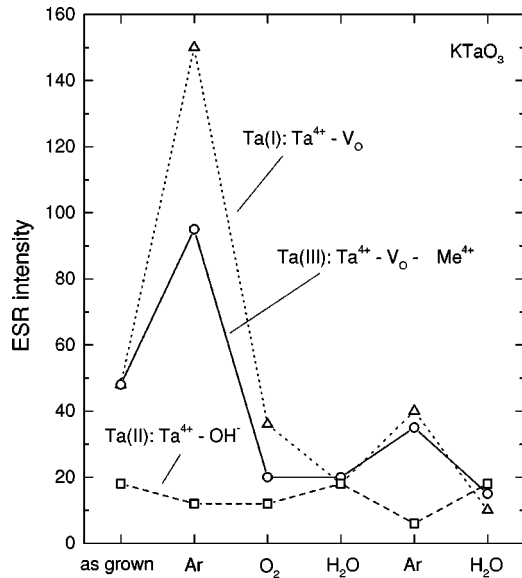


FIG. 8. The dependence of ESR intensity of Ta^{4+} centers on the annealing of $KTaO_3$ in Ar, O_2 and H_2O atmospheres.

vapors. In contrast, the intensity of the Ta(II) center decreased at the annealing in Ar atmosphere and increased in H_2O vapors. Note that we also tried to anneal samples in a H_2 atmosphere. However, it appeared impossible to measure ESR spectra accurately in the latter case because of strongly increasing dielectric losses at the ESR spectrometer frequency 9 GHz. The qualitative result was that the relative changes of ESR intensities were approximately the same as for annealing in H_2O vapor.

D. Models of Ta^{4+} centers in $KTaO_3$

The obtained experimental data made it possible to propose models of Ta^{4+} centers in $KTaO_3$. Let us analyze them. The increasing of concentration of the Ta(I) and Ta(III) centers after the annealing in an Ar atmosphere gives evidence that these centers contain vacancies. These can be oxygen vacancies, because the number of these centers decreases after annealing the sample in oxygen atmosphere. The simplest structure of these centers could be a complex involving an oxygen vacancy and two nearest Ta^{5+} ions, shifted from the centers of their oxygen octahedra. A local rearrangement of the nearest neighbor of the oxygen vacancy was suggested for the center $Ti^{3+}-V_O$ in $BaTiO_3$,²¹ with an estimated value of the titanium displacement of 0.35 Å. The displacement of the Fe^{3+} impurity for the $Fe^{3+}-V_O$ center as well as that of the oxygen atoms in the Ti (Ta) plane in $SrTiO_3$ was obtained in Ref. 22, and for $KTaO_3$ in Ref. 23. The rearrangement of lattice ions in the vicinity of V_O can be considered as the potential well for carrier trapping. One can assume that, similarly to Ref. 13, this well depth is small enough so that the photoelectron energy level can be shallow, i.e., it will be situated near the bottom of the conduction band. We guess that the electron trapped by the oxygen vacancy for the sake of charge compensation can be localized on a d_{xy} orbital of one out of the two nearest Ta^{5+} ions, creating a paramagnetic center $Ta^{4+}-V_O$ [Fig. 9(a)]. The localization of the electron on Ta^{5+} instead of localization on the V_O lattice site follows from g -factor values, which are typical for $5d^1$ ions

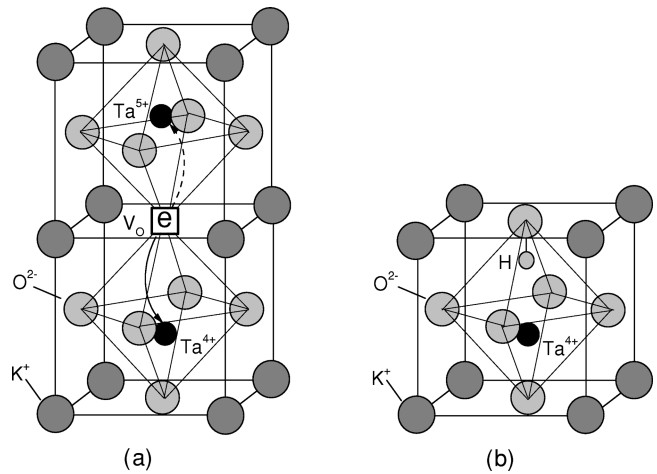


FIG. 9. The models of Ta^{4+} centers in $KTaO_3$ derived from ESR data: (a) $Ta^{4+}-V_O$; (b) $Ta^{4+}-OH^-$.

(see Table I). In the case of electron localization on the oxygen vacancy (F -center model) one can expect g -factor values close to that of free electron $g_s = 2.00$, because in this case $L = 0$ and $S = \frac{1}{2}$.

The possibility of electron localization on one of the Ta^{5+} ions nearest to the oxygen vacancy was recently predicted and calculated by Prosandeyev.²⁴ In particular, it was shown that under some conditions the energy of the complex $Ta^{4+}-V_O^{2+}-Ta^{5+}$ is lower than that of $Ta^{5+}-V_O^+-Ta^{5+}$. In this model Ta^{4+} and Ta^{5+} are shifted outward from V_O by 0.067 and 0.055 Å, respectively.

Let us emphasize that we can discuss an electron localization on one of the tantalum ions only on the ESR time scale $t \sim 10^{-9} - 10^{-10}$ s. The electron can obviously be localized on both of the tantalum ions with equal probability because of cubic lattice symmetry of $KTaO_3$ [see Fig. 9(a)]. One can assume thermal jumping of the electron between these equivalent positions. These jumps could manifest themselves in a dielectric susceptibility and in a broadening of the ESR line with an increase of temperature. Unfortunately, due to the high value of the dielectric constant, it was impossible to record the spectra in the temperature range 5–30 K, where this broadening could occur. The $Ta^{4+}-V_O$ center has an electric dipole moment of $d \approx 2e$ Å, thus it is a symmetry-breaking defect, contrary to the ‘pure’ oxygen vacancy without a trapped electron. On the other hand, an electron captured near sixfold-coordinated V_O in MgO (Ref. 25) or CaO ²⁶ does not break the cubic symmetry.

We assume that this model corresponds to the Ta(I) paramagnetic center on the basis of the following experimental facts. It is well known that in both $KTaO_3$ and $SrTiO_3$ the impurity ions of transition metals are associated to oxygen vacancies forming pair defects $Me^{x+}-V_O$ (Refs. 22 and 23) for charge compensation. That is why the number of $Ta^{4+}-V_O$ centers has to be smaller in crystals with such impurities than in purer crystals. The comparison of ESR intensities in two crystals, grown from starting materials (K_2CO_3 and Ta_2O_3) of high purity (first sample) and the highest commercially available purity (second sample), confirmed our assumption, showing, in the second sample, a strong increase (more than ten times) of the Ta(I) signal intensity in comparison with that of Ta(III). Note that usually the inten-

sity of ESR lines of Ta(I) and Ta(III) centers was approximately the same (see, e.g., Fig. 1).

The influence of annealing in various gas atmospheres on the ESR intensity of the Ta(III) center led us to the conclusion that, also for this center, its model has to incorporate an oxygen vacancy. It could be assumed that the Ta(III) center also includes, in addition to an oxygen vacancy, a vacancy of K⁺ (V_K) or some Me⁴⁺ impurity ion substituted for Ta⁵⁺. The latter seems to be more probable because of the axial symmetry of the center. The Me⁴⁺ impurities could be Sn⁴⁺ or Ti⁴⁺ ions, a small amount of which was revealed by the electron-microprobe method in the sample with the most intensive Ta(III) spectrum. After illumination, the Ta(III) center (Ta⁴⁺-V_O-Me⁴⁺) is completely compensated for, while the compensation of the net positive charge of the Ta(I) center (Ta⁴⁺-V_O) can be due to the V_K presence in the distant spheres. The Ta(III) centers have an electric dipole moment so that they are symmetry-breaking defects in the KTaO₃ lattice.

The Ta(II) is not connected with oxygen vacancies because of the results depicted in Fig. 7. The increased concentration of these centers after annealing in water vapors indicates a connection of these centers with OH⁻ groups. These groups are known to be unavoidable defects in KTaO₃, as was shown earlier by infrared measurements.¹¹ We guess that in the Ta(II) centers the OH⁻ molecule is situated on an oxygen site. The axial symmetry of Ta(II) centers along ⟨001⟩ directions confirms this supposition. If the OH⁻ group was an interstitial defect, situated either between two K⁺ ions or between K⁺ and Ta⁵⁺, its symmetry would be axial but along the ⟨011⟩ or ⟨111⟩ directions, respectively. Other interstitial positions of OH⁻ seem to be less probable because they lead to substantial lattice perturbations. Moreover, the investigation of the infrared spectra, performed after crystal annealing in both water vapors and in H₂ atmosphere, had shown that hydrogen diffusion (rather than diffusion of whole OH⁻ molecules) takes place in the crystal.^{11,27} At high temperatures, hydrogen jumps from one oxygen to another. At low temperatures, the thermal energy is not enough for such jumping, so the hydrogen ion localizes in the vicinity of an O²⁻ ion, creating an OH⁻ molecule. Since the OH⁻ molecule has an intrinsic electric dipole moment, it induces an asymmetric lattice distortion, so that the two nearest Ta⁵⁺ ions become inequivalent. As a result, one out of two inequivalent Ta⁵⁺-OH⁻ configurations with excessive positive charge can trap a photoelectron and transform into a paramagnetic Ta⁴⁺-OH⁻ complex, which is completely charge compensated. Such a center has an electric dipole moment, so it is a symmetry-breaking defect in the KTaO₃ lattice. The proposed model of the center is depicted in Fig. 9(b). In this model we suppose that Ta⁵⁺ is shifted from OH⁻, which substitutes for the nearest oxygen ion. This is because the latter molecular ion, similarly to the oxygen vacancy, has an effective positive charge in the lattice and a size larger than that of the oxygen ion.²⁸ The proton position in the Ta(II) center is not clear. However, the proton is assumed to be situated between the O²⁻ and Ta⁴⁺ ions [as depicted in Fig. 9(b)] due to the tetragonal symmetry of the center. Note that the proton could be repelled by the Ta⁵⁺ ion before the latter traps the electron. In this state, the proton may occupy some other position between two O²⁻ ions.

IV. DISCUSSION AND CONCLUSION

Various Ta⁴⁺ centers (Ta⁴⁺-V_O, Ta⁴⁺-OH⁻, and Ta⁴⁺-V_O-Me⁴⁺) have been studied and identified after sample illumination by photons with an energy close to the band gap of KTaO₃, as the consequence of electron capture near an oxygen vacancy or OH⁻ molecule. Their local electronic levels were shown to lie very close to the bottom of the conduction band. At $T \geq 30$ K, the majority of these centers are ionized and transformed into V_O and OH⁻, which are supposed to be the main lattice defects before illumination. The small ionization energies of the centers seem to be the consequence of the large dielectric permittivity ϵ of KTaO₃ (about 3000–4000 at $T \leq 30$ K). The energy of the trapped electron is proportional to $1/\epsilon$, i.e., it has to be small at $T \leq 30$ K. It is much less than that of the similar electron center Ti³⁺-V_O in BaTiO₃.²¹ It is interesting to note that, in SrTiO₃, where the dielectric permittivity has approximately the same value, no Ti³⁺-V_O center has been observed after reduction, optical, x-ray, or neutron irradiation.²⁹ Moreover, the Ta⁴⁺ centers did not appear in KTaO₃ with even one percent of Nb⁵⁺ impurity. These facts point to a high sensitivity of local energy levels of tantalum (titanium) ions to fine details of host lattice band structures, which in the case of KTaO₃:Nb might be slightly different.

The most important thing is that all three Ta⁴⁺ centers have electric dipole moments $d \approx 2e \text{ \AA}$, i.e., they can be the sources of polar cluster formation in illuminated KTaO₃. The electric dipole moments of Ta⁴⁺-V_O centers look like those of O⁻-Al³⁺ centers in SiO₂:Al, where the hole is trapped on one out of two equivalent O²⁻ ions, which are the nearest neighbors of an Al³⁺ ion substituting for Si⁴⁺. These O⁻-Al³⁺ centers are known to appear only in x-ray-irradiated samples, and are “responsible” for many anomalous properties of SiO₂:Al.³⁰

We have to emphasize that, in addition to the photoinduced electric dipole moment of Ta⁴⁺-OH⁻ centers, the OH⁻ molecules may also have intrinsic dipole moments originating from their asymmetry and possible off-center position in the oxygen site, similarly to the case of potassium chloride.³¹ Our estimation of OH⁻ concentration, based on an integral intensity calculation of the Ta⁴⁺-OH⁻ ESR spectrum, gives 10^{18} – 10^{19} cm^{-3} , which is close to the concentration of symmetry-breaking defects obtained in Ref. 10 on the basis of SHG intensity evaluation. It is obvious that hydrogen-based defects should always be present in a crystal fabricated in an ordinary atmosphere containing H₂O vapors. The other two Ta⁴⁺ centers, including the oxygen vacancy, can also contribute to the intensity of SHG and first-order Raman scattering, because for such measurements intensive laser light is applied. This illumination can generate photoelectrons in the conduction band due to two-phonon excitation from the valence band via deep impurity levels (e.g., Fe³⁺, Gd³⁺, and Mn²⁺), similarly to the process described in Ref. 13. The trapping of the photoelectrons has to result in the emergence of symmetry-breaking Ta⁴⁺-V_O and Ta⁴⁺-V_O-Me⁴⁺ centers.

In the last few years there has been discussion in the literature about Ta³⁺-V_O centers as unavoidable symmetry-

breaking defects in KTaO_3 (see, for instance, Ref. 6). Earlier, these centers were assumed to be the main reason for large conductivity in KTaO_3 samples. The conductivity appears at some definite regimes of crystal growth. It can also occur in a thin surface layer of insulating crystals after several hours' exposure in hydrogen atmosphere at $T \approx 900\text{--}1000^\circ\text{C}$.^{12,32} The crystals obtained in such a manner had a deep blue color, and a carrier concentration in the range $5 \times 10^{17}\text{--}10^{19}\text{ cm}^{-3}$ ($\rho \approx 1\text{--}0.02\ \Omega\ \text{cm}$). In contrast, the reduction of bulk insulating KTaO_3 crystals in hydrogen keeps them colorless and highly resistant. Under these conditions, the concentration of symmetry-breaking defects increased in 2-h treatment from 8×10^{17} to $4 \times 10^{18}\text{ cm}^{-3}$.¹⁰ This contradiction seems to be due to a difference in concentration and types of the defects appearing in thin layers and bulk samples of KTaO_3 during reduction in hydrogen. On the other hand, the results of our measurements (see Sec. III), as well as OH^- absorption in bulk samples^{11,27} show the increase of OH^- concentration rather than that of V_{O} under annealing in H_2 . Only after saturation of the sample with hydrogen, which takes place in the first 3–4 h of the annealing at $T \approx 1000^\circ\text{C}$, large enough numbers of V_{O} can appear. The latter process, in contrast to diffusion of hydrogen, has small velocity. In thin layers the diffusion process, especially reduction, is much faster. As a result, in thin layers V_{O} creation can be the prevailing process from the very beginning of annealing. It was shown in previous sections that V_{O} with a trapped electron leads to the appearance of a $\text{Ta}^{4+}\text{-}V_{\text{O}}$ (or $\text{Ta}^{4+}\text{-}V_{\text{O}}\text{-Me}^{4+}$) center, its electronic level being 0.026 eV (0.008 eV). Therefore, at least at $T < 30\text{ K}$ these centers cannot contribute to electron current. However, such current was observed for temperatures as low as 1.6 K.¹² It seems that

some donor centers like V_{O} with two trapped electrons ($V_{\text{O}}^{\bullet\bullet}$) in reduced KTaO_3 can be considered as the source of electrons in a current. A simple hydrogenlike donor model predicts a very small electron ionization energy ($\approx 10^{-4}\text{ eV}$) for the $V_{\text{O}}^{\bullet\bullet}$. In addition, for $\varepsilon > 1000$, the radius of an electron orbital is comparable with the average distance between donor centers (100–150 Å), so that an impurity band might be formed. This band could overlap with the conduction band. As a result the conductivity will occur even at the lowest temperatures.

The Ta^{4+} centers are shown to be shallow donors, so they can influence the low-temperature photoconductivity in KTaO_3 . Indeed, in the samples of $\text{KTaO}_3\text{:Nb}$, where the photoinduced centers were not observed, we measured a drastic decrease of the photocurrent at $T \leq 100\text{ K}$, up to its complete disappearance.³³ Contrary to this, in KTaO_3 , where the photoinduced centers are present, the photocurrent at $T \leq 100\text{ K}$ is anomalously large.

Finally, we want to point out that dipolar Ta^{4+} symmetry-breaking defects, formed on the basis of cubic-symmetry oxygen vacancies, can be of great importance for solving a puzzle about the observation of phenomena like SHG and FOR which must be absent in cubic lattices. Additional experimental studies of these centers, with the help of optical absorption, dielectric spectroscopy, and electron-nuclear double resonance, as well as calculations of their electronic structure and crystal fields, would be desirable in the future.

ACKNOWLEDGMENTS

The authors would like to thank A. Cihlař for his fruitful help with the annealing procedure, Dr. I. M. Smolyaninov for helpful discussions, and Dr. V.A. Stephanovich for a critical reading of the manuscript.

-
- ¹M. D. Glinchuk, V. V. Laguta, I. P. Bykov, J. Rosa, and L. L. Jastrabik, *J. Phys.: Condens. Matter* **7**, 2605 (1995).
- ²A. P. Pechenyi, M. D. Glinchuk, C. Azzoni, F. Scardina, and A. Paleari, *Phys. Rev. B* **51**, 12 165 (1995).
- ³W. Prusseit-Elffroth and F. Schwabl, *Appl. Phys. A: Solids Surf.* **51**, 361 (1990).
- ⁴H. Uwe, K. B. Lyons, H. L. Carter, and P. A. Fleury, *Phys. Rev. B* **33**, 6436 (1986).
- ⁵B. Salce, J. L. Graviil, and L. A. Boatner, *J. Phys.: Condens. Matter* **6**, 4077 (1994).
- ⁶P. Grenier, G. Bernier, S. Jandl, and L. A. Boatner, *J. Phys.: Condens. Matter* **1**, 2515 (1989).
- ⁷S. Jandl, M. Banville, P. Dufour, and S. Coulombe, *Phys. Rev. B* **43**, 7555 (1991).
- ⁸S. A. Prosandeyev and I. A. Osipenko, *Phys. Status Solidi B* **192**, 37 (1995).
- ⁹H. Vogt, *J. Phys.: Condens. Matter* **3**, 3697 (1991).
- ¹⁰C. Fischer, C. auf der Horst, P. Voigt, S. Kapphan, and J. Zhao, *Radiat. Eff. Defects Solids* **136**, 85 (1995).
- ¹¹H. Engstrom, J. B. Bates, and L. A. Boatner, *J. Chem. Phys.* **73**, 1073 (1980).
- ¹²S. H. Wemple, *Phys. Rev.* **137**, A1575 (1965).
- ¹³R. S. Klein, G. E. Kugel, M. D. Glinchuk, R. O. Kuzian, and I. V. Kondakova, *Phys. Rev. B* **50**, 9721 (1994).
- ¹⁴V. V. Laguta, M. D. Glinchuk, I. P. Bykov, M. I. Zaritskii, J. Rosa, L. Jastrabik, V. Trepakov, and P. P. Syrnikov, *Solid State Commun.* **98**, 1003 (1996).
- ¹⁵V. V. Laguta, M. D. Glinchuk, I. P. Bykov, J. Rosa, L. Jastrabik, R. S. Klein, and G. E. Kugel, *Phys. Rev. B* **52**, 7102 (1995).
- ¹⁶A. Abraham and B. Bleaney, *Electron Paramagnetic Resonance of Transition Ions* (Clarendon, Oxford, 1970).
- ¹⁷K. A. Müller, Th. von Waldkirch, W. Berlinger, and B. W. Fanghnan, *Solid State Commun.* **9**, 1097 (1971).
- ¹⁸I. N. Geifman, *Phys. Status Solidi B* **85**, k5 (1978).
- ¹⁹R. Bube, *Photoconductivity of Solids* (Wiley, New York, 1960).
- ²⁰E. Possenriede *et al.*, *Ferroelectrics* **151**, 199 (1994).
- ²¹R. Scharfschwerdt, A. Mazur, O. F. Schirmer, H. Hesse, and S. Mendricks, *Phys. Rev. B* **54**, 15 284 (1996).
- ²²E. Siegel and K. A. Müller, *Phys. Rev. B* **19**, 109 (1979).
- ²³I. P. Bykov, M. D. Glinchuk, A. A. Karmazin, and V. V. Laguta, *Fiz. Fverd. Tela (Leningrad)* **25**, 3586 (1983) [*Sov. Phys. Solid State* **25**, 2063 (1983)].
- ²⁴S. A. Prosandeyev, *Zh. Éksp. Teor. Fiz.* **110**, 1355 (1983) [*JETP* **83**, 747 (1996)].
- ²⁵B. Henderson and J. E. Wertz, *Electron Spin Resonance: Elementary Theory and Practical Applications* (Taylor & Francis, London, 1977).

- ²⁶W. B. Fowler, *Physics of Color Centers* (Academic, New York, 1968).
- ²⁷R. Gonzalez, M. M. Abraham, L. A. Boatner, and J. Chen, *J. Chem. Phys.* **78**, 660 (1983).
- ²⁸N. Sata, K. Hiramoto, M. Ishigame, S. Hosoya, N. Niimura, and S. Shin, *Phys. Rev. B* **54**, 15 795 (1996).
- ²⁹K. A. Müller, W. Berlinger, and R. S. Rubins, *Phys. Rev.* **186**, 361 (1969).
- ³⁰W. J. De Vos and J. Volger, *Physica (Amsterdam)* **47**, 13 (1970).
- ³¹U. T. Fiory, *Phys. Rev. B* **4**, 614 (1970).
- ³²D. M. Hannon, *Phys. Rev.* **164**, 366 (1967).
- ³³V. V. Laguta *et al.* (unpublished).